1-1-2011

Numerical modeling of alkali vapor lasers

Hong Shu
University of Central Florida

Ying Chen
University of Central Florida

Michael Bass
University of Central Florida

Fernando Monjardin

Jochen Deile

Numerical modeling of alkali vapor lasers

Hong Shu,[1*] Ying Chen,[1] Michael Bass,[1] J. Fernando Monjardin,[2] and Jochen Deile[2]

[1]*College of Optics and Photonics, CREOL, FPCE, and Townes Laser Institute, University of Central Florida, Orlando, Florida 32816, USA*

[2]*TRUMPF Inc., 5 Johnson Ave, Farmington, Connecticut 06032, USA*

**hshu@creol.ucf.edu*

Abstract: Detailed numerical analyses are presented of a continuous wave (cw), single spatial mode alkali vapor laser pumped by a diffraction-limited Ti: Sapphire laser. These analyses provide insight into the operation of alkali vapor lasers to aid in the development of high power, diode laser pumped alkali vapor lasers. It is demonstrated that in the laser considered the laser spatial pattern is significantly changed after each pass through the gain medium, and the laser spatial pattern in steady state operation is also very different from that of the passive cavity mode. According to the calculation, lasing significantly improves the pump absorption efficiency and changes the absorbed pump distribution. The effect of varying the transverse size of the pumped region is also analyzed and an optimum pump beam waist radius is demonstrated. In addition, the shift of the pump beam waist location is also studied. The computation method and its convergence behavior are also described in detail.

OCIS codes: (140.1340) Atomic gas lasers; (140.3430) Laser theory; (140.3410) Laser resonators; (000.4430) Numerical approximation and analysis.

References

1. R. J. Beach, W. K. Krupke, V. K. Kanz, S. A. Payne, M. A. Dubinskii, and L. D. Merkle, "End-pumped continuous-wave alkali vapor lasers: experiment, model, and power scaling," J. Opt. Soc. Am. B **21**(12), 2151–2163 (2004).
2. W. F. Krupke, R. J. Beach, V. K. Kanz, and S. A. Payne, "Resonance transition 795-nm rubidium laser," Opt. Lett. **28**(23), 2336–2338 (2003).
3. B. V. Zhdanov, T. Ehrenreich, and R. J. Knize, "Highly efficient optically pumped cesium vapor laser," Opt. Commun. **260**(2), 696–698 (2006).
4. B. V. Zhdanov and R. J. Knize, "Diode-pumped 10 W continuous wave cesium laser," Opt. Lett. **32**(15), 2167–2169 (2007).
5. S. S. Q. Wu, T. F. Soules, R. H. Page, S. C. Mitchell, V. K. Kanz, and R. J. Beach, "Hydrocarbon-free resonance transition 795-nm rubidium laser," Opt. Lett. **32**(16), 2423–2425 (2007).
6. A. Gourevitch, G. Venus, V. Smirnov, D. A. Hostutler, and L. Glebov, "Continuous wave, 30 W laser-diode bar with 10 GHz linewidth for Rb laser pumping," Opt. Lett. **33**(7), 702–704 (2008).
7. H. Shu and M. Bass, "Three-dimensional computer model for simulating realistic solid-state lasers," Appl. Opt. **46**(23), 5687–5697 (2007).
8. H. Shu, Analytic and numeric modeling of diode laser pumped Yb:YAG laser oscillators and amplifiers, Ph.D dissertation (University of Central Florida, 2003).
9. W. P. Risk, "Modeling of longitudinally pumped solid-state lasers exhibiting reabsorption losses," J. Opt. Soc. Am. B **5**(7), 1412–1423 (1988).
10. T. Y. Fan and R. L. Byer, "Modeling and CW Operation of a Quasi-Three-Level 946 nm Nd: YAG Laser," IEEE J. Quantum Electron. **23**(5), 605–612 (1987).
11. W. Koechner, *Solid-State Laser Engineering* (Springer, 1999).
12. W. F. Krupke and L. L. Chase, "Ground-state depleted solid-state lasers: principles, characteristics and scaling," Opt. Quantum Electron. **22**(S1), S1–S22 (1990).
13. F. Sanchez, M. Brunel, and K. Ait-Ameur, "Pump-saturation effects in end-pumped solid-state lasers," J. Opt. Soc. Am. B **15**(9), 2390–2394 (1998).
14. Y. Sato and T. Taira, "Saturation Factors of Pump Absorption in Solid-State Lasers," IEEE J. Quantum Electron. **40**(3), 270–280 (2004).
15. Z. Konefał, "Observation of collision induced processes in rubidium-ethane vapour," Opt. Commun. **164**(1-3), 95–105 (1999).
16. A. E. Siegman, "Gain-guided, index-antiguided fiber lasers," J. Opt. Soc. Am. B **24**(8), 1677–1682 (2007).

#152299 - $15.00 USD Received 3 Aug 2011; revised 2 Sep 2011; accepted 3 Sep 2011; published 26 Sep 2011

17. Y. Chen, T. McComb, V. Sudesh, M. Richardson, and M. Bass, "Very large-core, single-mode, gain-guided, index-antiguided fiber lasers," Opt. Lett. **32**(17), 2505–2507 (2007).

1. Introduction

Recently alkali vapor lasers have been reported [1]-[5]. Alkali vapor lasers are three level lasers with the advantage of small quantum defect. In addition, they can be pumped by diode lasers with linewidth narrowed using, for example, volume Bragg gratings [6], and narrowing of the linewidth for the pump excitation is important for diode laser pumped alkali vapor lasers. In [1] the physical processes involved in alkali vapor lasers were investigated in detail.

In this paper, the application of a numerical model initially developed for analyzing solid state lasers [7], [8] is presented for analyzing a single spatial mode alkali vapor laser. The analysis properly accounts for the physical processes in this type of three level laser that differ from those in the quasi three level solid state lasers considered in [7], [8], [9], [10]. When applied to the single spatial mode Cs laser pumped by a diffraction limited Ti:Sapphire laser presented in [1], the model gives good agreement with the experimental results. It also shows that in steady state cw operation the laser spatial pattern is significantly reshaped after each pass through the Cs gain medium, and the laser spatial pattern in steady state operation is very different from that of the TEM_{00} mode of the passive cavity. In addition, the calculation shows that laser operation can significantly improve the pump absorption efficiency and change the absorbed pump distribution. The effect of varying the transverse size of the pumped region was also analyzed, and an optimum pump beam waist radius is demonstrated, for which the laser efficiency is maximized for the specific laser set-up. The effect of pump beam waist location shift was also studied. First, the computation method will be described in the coming section.

2. Computation method

A computational model initially developed for analyzing solid state lasers [7], [8] was applied for the analyses presented in this paper. This model includes ground state depletion in quasi three level solid state lasers by further iteration between the calculation for the TEM_{00} Gaussian pump laser and the calculation for the signal laser [8]. In the model, the counter propagating two beams (also applicable to more than two beams) in an active laser cavity with saturated gain medium is treated by a simple iteration of the beam propagation method (BPM) calculation [7], [8]. Of course, if there is only one beam passing through the gain medium in a single pass, the iteration of BPM calculation is not necessary. For a laser cavity with an intracavity polarizer the laser beam can be assumed to be linearly polarized and the scalar formulation of the beam propagation method described in [7] suffices.

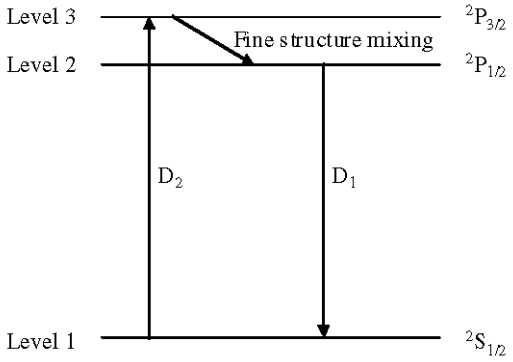

Fig. 1. Schematic energy level diagram for alkali metal vapors.

Unlike the 1030 nm laser transition for Yb:YAG considered in [7] or the 946 nm laser transition for Nd:YAG considered in [9] and [10], the alkali vapor lasers including Cs and Rb lasers are three level systems. The energy levels in alkali vapors are shown in Fig. 1. Using

#152299 - $15.00 USD Received 3 Aug 2011; revised 2 Sep 2011; accepted 3 Sep 2011; published 26 Sep 2011

the rate equations described in [1] and the notation described in [8], the rate equations for both the pump and laser transitions in alkali vapor lasers are

$$\begin{aligned}
\frac{dN_3}{dt} &= \frac{\sigma_p\left(N_1-\frac{1}{2}N_3\right)\cdot I_p}{h\nu_p} - \gamma_{3\to 2}\cdot N_3 + \gamma_{3\to 2}\cdot 2\cdot e^{-\frac{\Delta E}{k_B T}}\cdot N_2 - \frac{N_3}{\tau_3} \\
\frac{dN_2}{dt} &= -\sigma(N_2-N_1)\cdot\frac{I}{h\nu_L} + \gamma_{3\to 2}\cdot N_3 - \gamma_{3\to 2}\cdot 2\cdot e^{-\frac{\Delta E}{k_B T}}\cdot N_2 - \frac{N_2}{\tau_2} \\
\frac{dN_1}{dt} &= -\frac{\sigma_p\left(N_1-\frac{1}{2}N_3\right)\cdot I_p}{h\nu_p} + \sigma(N_2-N_1)\cdot\frac{I}{h\nu_L} + \frac{N_2}{\tau_2} + \frac{N_3}{\tau_3}
\end{aligned} \tag{1}$$

Note that Eqs. (1) apply to any specific spatial position in the gain medium and N_1, N_2, N_3, I, I_p, T could vary with space coordinates x, y, and z. Here N_1, N_2 and N_3 are the population densities in levels 1, 2 and 3 respectively, $\gamma_{3\to 2}$ is the fine structure mixing rate due to the collision of the alkali atoms with ethane [1] or He [5] buffer gases, τ_2 is the radiative lifetime for the upper laser level, τ_3 is the radiative lifetime for the upper pump level, ν_L is the frequency of the laser, ν_p is the frequency of the pump. I is the total intensity of the laser beam including the two counter propagating laser beams. It is assumed that $I = I^+ + I^- = I^+(x,y,z) + I^-(x,y,z)$ similar to the treatment in [7]. Here I^+ and I^- denote the intensities of the two counter propagating laser beams in the gain medium. I_p is the total intensity of the pump beam. If the pump beam passes through the gain medium for two passes in opposite directions such as the case described in [8], I_p is expressed as $I_p = I_p^+ + I_p^- = I_p^+(x,y,z) + I_p^-(x,y,z)$, where I_p^+ and I_p^- denote the intensities of the two counter propagating pump beams in the gain medium. If the pump beam passes through the gain medium for one single pass, the pump intensity is simply I_p without the counter propagating beam. ΔE is the energy gap between the upper pump level and upper laser level, T is the absolute temperature of the alkali vapor, σ is the collision broadened line-center emission cross section assuming homogeneous broadening, σ_p is the average of the collision broadened pump absorption cross section through the pump spectral profile.

Alkali vapor lasers are gas lasers. In gas lasers spatial hole burning could be reduced by the thermal motions of the atoms [11]. In alkali vapor lasers however, due to high excited state fractions during laser operation, the thermal motions of the atoms might not be able to remove spatial hole burning completely. Therefore, multiple longitudinal modes might still lase simultaneously as is similar to the case of solid state lasers discussed in [7]. In [7] more discussions on spatial hole burning and multiple longitudinal modes can be found.

In steady state cw operation all the time derivatives in Eqs. (1) are zero and the following solution can be obtained

#152299 - $15.00 USD Received 3 Aug 2011; revised 2 Sep 2011; accepted 3 Sep 2011; published 26 Sep 2011

$$N_1 = \frac{\dfrac{\sigma_p I_p}{2h\nu_p} + \gamma_{3\to 2} + \dfrac{1}{\tau_3} - \dfrac{\dfrac{\sigma_p I_p}{2h\nu_p} + \gamma_{3\to 2}\cdot 2\cdot e^{-\frac{\Delta E}{k_B T}} + \gamma_{3\to 2} + \dfrac{1}{\tau_3}}{\dfrac{\sigma I}{h\nu_L} + \gamma_{3\to 2}\cdot 2\cdot e^{-\frac{\Delta E}{k_B T}} + \gamma_{3\to 2} + \dfrac{1}{\tau_2}}\cdot \gamma_{3\to 2}}{\dfrac{3\sigma_p I_p}{2h\nu_p} + \gamma_{3\to 2} + \dfrac{1}{\tau_3} + \dfrac{\dfrac{\sigma_p I_p}{2h\nu_p} + \gamma_{3\to 2}\cdot 2\cdot e^{-\frac{\Delta E}{k_B T}} + \gamma_{3\to 2} + \dfrac{1}{\tau_3}}{\dfrac{\sigma I}{h\nu_L} + \gamma_{3\to 2}\cdot 2\cdot e^{-\frac{\Delta E}{k_B T}} + \gamma_{3\to 2} + \dfrac{1}{\tau_2}}\cdot\left(\dfrac{\sigma I}{h\nu_L} - \gamma_{3\to 2}\right)}\cdot N_0$$

$$N_2 = \frac{\left(\dfrac{\sigma I}{h\nu_L} - \gamma_{3\to 2}\right)\cdot N_1 + \gamma_{3\to 2}\cdot N_0}{\dfrac{\sigma I}{h\nu_L} + \gamma_{3\to 2}\cdot 2\cdot e^{-\frac{\Delta E}{k_B T}} + \gamma_{3\to 2} + \dfrac{1}{\tau_2}} \qquad (2)$$

$$N_3 = N_0 - N_1 - N_2$$

Here N_0 is the total alkali number density. The saturated laser gain coefficient can then be written as

$$g(x,y,z) = \sigma\cdot\left(N_2 - N_1\right) = \sigma\cdot\left\lfloor N_2(x,y,z) - N_1(x,y,z)\right\rfloor \qquad (3)$$

where N_1 and N_2 are expressed in (2).

Ground state depletion is an important issue for alkali vapor lasers. Ground state depletion was discussed previously for solid state lasers [8], [12], [13], [14]. Some of the physical processes that are relevant to laser operation in Rb vapor are also discussed in [15], which can serve as a further confirmation of the rate equations shown in Eqs. (1). Similar to the treatment in [8], the propagation of the pump beam is also calculated using the beam propagation method. The beam propagation method is expected to be accurate for the pump beam considered in this paper, a Ti: Sapphire laser operating in the TEM_{00} spatial mode. The saturated absorption coefficient for the pump is

$$\alpha_p(x,y,z) = \sigma_p\cdot\left(N_1 - \frac{1}{2}\cdot N_3\right) = \sigma_p\cdot\left\lfloor N_1(x,y,z) - \frac{1}{2}\cdot N_3(x,y,z)\right\rfloor \qquad (4)$$

where N_1 and N_3 are calculated according to Eqs. (2). As stated in [1] the relative degeneracies of levels 1 and 3 are 2 and 4, respectively, and this is the reason for the factor of $1/2$ in Eqs. (4) and (1). The presence of this factor of $1/2$ also agrees with the discussion presented in [15].

In [7] the iteration of the beam propagation calculation is conducted only for the laser beam since ground state depletion is neglected for the Yb:YAG gain medium at 77 K. In [8] the iteration of the beam propagation calculation for the pump laser is further iterated with the iteration of the beam propagation calculation for the signal laser to include ground state depletion.

In alkali vapor lasers ground state depletion is very important and has to be included. Therefore, similar to the treatment in [8], the iteration of the beam propagation calculation for the TEM_{00} Gaussian mode pump laser must be further iterated with the iteration of the beam propagation calculation for the signal laser. During the iteration calculation the saturated laser gain coefficient used is that in Eq. (3) and the saturated pump absorption coefficient used is that in Eq. (4).

#152299 - $15.00 USD Received 3 Aug 2011; revised 2 Sep 2011; accepted 3 Sep 2011; published 26 Sep 2011

As a general strategy, the iteration between the calculation for the pump laser and the calculation for the signal laser can be done using the procedure shown below. The iteration procedure could vary a little bit especially in the starting stage. The signal laser can start from any arbitrarily chosen field amplitude for the iteration calculation, and the initial choice of the field amplitude of the signal laser used for the calculation affects the number of iteration steps needed to reach a specific accuracy. The iteration procedure is as follows:

(a) First, set the intensities for the two counter propagating signal laser beams $I^{+}(x,y,z)$ and $I^{-}(x,y,z)$ to zero anywhere inside the gain medium, as the initial condition. The pump laser is numerically propagated through the gain medium once (one single pass or multiple passes depending on the pump set-up). For a TEM_{00} Gaussian pump laser which is the case considered in this paper, the beam propagation method is suitable. If the pump beam passes through the gain medium for two passes in opposite directions, the iteration of the beam propagation calculation can be used. For this calculation, the saturated pump absorption coefficient shown in Eq. (4) needs to be used and it can be included in the paraxial wave equation in a straightforward way. In Eq. (4) N_1 and N_3 are expressed in Eqs. (2). After the calculation is finished (or at some particular stages during the iteration calculation as are similar to the description in [7]), the complex amplitude of the electric field for the pump laser anywhere inside the gain medium is properly stored.

(b) The signal laser, starting from an arbitrary field amplitude, is numerically propagated through the cavity for one round trip, using the iteration of the beam propagation calculation [7]. For this calculation, the saturated laser gain coefficient shown in Eq. (3) needs to be used and it is included in the paraxial wave equation in the way described in [7] and [8]. In Eq. (3) N_1 and N_2 are expressed in Eqs. (2). For this calculation, the numerical value of the total pump laser intensity $I_p(x,y,z)$ is calculated using the complex amplitude of the electric field for the pump laser stored in the previous step. After the calculation is finished (or at some particular stages during the iteration calculation as are similar to the description in [7]), the complex amplitudes of the electric fields for the two counter propagating laser beams anywhere inside the gain medium are properly stored.

(c) The pump laser is numerically propagated through the gain medium once again (one single pass or multiple passes depending on the pump set-up). Again, for this calculation, the saturated pump absorption coefficient shown in Eq. (4) needs to be used, in which N_1 and N_3 are expressed in Eqs. (2). The numerical value of the total laser intensity $I(x,y,z)=I^{+}(x,y,z)+I^{-}(x,y,z)$ is calculated using the complex amplitudes of the electric fields for the two counter propagating laser beams stored in the previous step. After the calculation is finished (or at some particular stages during the iteration calculation as are similar to the description in [7]), the complex amplitude of the electric field for the pump laser anywhere inside the gain medium is properly stored.

(d) The signal laser is numerically propagated through the cavity for one more round trip, using the iteration of the beam propagation calculation [7]. Again, the saturated laser gain coefficient shown in Eq. (3) needs to be used, in which N_1 and N_2 are expressed in Eqs. (2). For this calculation, the numerical value of the total pump laser intensity $I_p(x,y,z)$ is calculated using the complex amplitude of the electric field for the pump laser stored in the previous step. After the calculation is finished (or at some particular stages during the iteration calculation as are similar to the

#152299 - $15.00 USD Received 3 Aug 2011; revised 2 Sep 2011; accepted 3 Sep 2011; published 26 Sep 2011

description in [7]), the complex amplitudes of the electric fields for the two counter propagating laser beams anywhere inside the gain medium are properly stored.

Steps (c) and (d) need to be repeated sequentially (in the sequence as steps (c), (d), (c), (d), …), until the solution converges to the desired accuracy.

It needs to be noted that although Eqs. (2), (3), and (4) are always used in the computation to include the saturated laser gain and saturated pump absorption, they only represent the correct solution when the computation eventually reaches convergence. The reason that Eqs. (2), (3), and (4) are used, even when they are far away from the correct solution when the computation is still far from converging to a specific accuracy, is because when convergence is eventually reached, they then truly represent the correct steady state solution within the specific accuracy of the numerical approximation. The same reasoning also applies to the paraxial wave equation for the BPM calculation. The practical numerical calculations presented in [7], [8], and this paper demonstrate that this method works very well for continuous wave (cw) lasers. It also works well for long-pulse lasers.

Using this type of iteration calculation, no convergence difficulty was encountered when analyzing active laser resonators with a single transverse mode (spatial mode) oscillating, and converged solution can generally be obtained quickly for modeling active laser resonators supporting only a single spatial mode, such as the active laser resonators considered in [7], [8], and this paper. On the other hand, if the considered active laser resonator supports more than one transverse modes lasing simultaneously, the convergence behavior of the computation is very different compared to that with only one transverse mode lasing. The in-depth analysis of these convergence behaviors has not been attempted yet, and the convergence behavior of the computation also needs more detailed investigation, especially for analyzing active laser resonators supporting more than one transverse mode. However, this convergence feature itself is very useful to tell if a specific laser design will operate in single transverse mode or multiple transverse modes.

This convergence feature might also be interesting when the computation method described here is applied for analyzing the gain guided, index antiguided fiber lasers [16], [17].

3. Numerical results and discussions

The numerical model described above was applied to analyze the Cs laser experiment described in [1]. The end-pumped 894.6 nm Cs laser pumped by an 852.3 nm Ti:Sapphire laser as sketched in Fig. 2 of Ref [1]. was analyzed in detail. In this laser the high reflector mirror is flat, and the output coupler mirror has a concave radius of 20 cm. The optical length of the laser cavity is 19.9 cm and the thicknesses of the Cs cell windows are neglected in the calculations. Between the right window of the Cs cell and the high reflector the distance was taken to be 2.5 cm. According to the description in [1] the length of the Cs gain medium was 2.5 cm along the laser axis. The refractive index of the Cs vapor was taken to be 1.0. The distance between the left window of the Cs cell and the output coupler was 14.9 cm. The material parameters used were those described in [1]. In [1], the Cs gain cell temperature was held at 110 ∫C, giving a Cs number density of $N_0 = 2.7\times10^{13}/cm^3$. In the present computation it was assumed that the temperature is uniformly 110 ∫C across the whole Cs gain medium. Consequently, the total Cs number density is uniformly $N_0 = 2.7\times10^{13}/cm^3$ across the whole Cs gain medium. σ as shown in Eqs. (1), (2) and (3) is $\sigma = 4.84\times10^{-13}\ cm^2$ which is the collision broadened line-center emission cross section for the laser transition. σ_p as used in Eqs. (1), (2) and (4) is $\sigma_p \cong 4.12\times10^{-13}\ cm^2$, which is the average of the collision broadened pump absorption cross section over the pump spectral profile. The fine structure mixing rate used in the computation is $\gamma_{3\to2} = 1.07\times10^9/s$. $\tau_2 = 34.9$ ns, $\tau_3 = 30.5$ ns, and $\Delta E = 554\ cm^{-1}$ as given in Ref [1].

#152299 - $15.00 USD Received 3 Aug 2011; revised 2 Sep 2011; accepted 3 Sep 2011; published 26 Sep 2011

Similar to the calculation in [7] the total intensity of the laser in the gain medium in Eqs. (1) and (2) is $I(x,y,z)=I^{+}(x,y,z)+I^{-}(x,y,z)$ where $I^{+}(x,y,z)$ and $I^{-}(x,y,z)$ denote the intensities of the two counter propagating laser beams in the gain medium. The iteration of the beam propagation calculation [7] was conducted to treat the signal laser propagation back and forth in the cavity containing the Cs gain cell. Since the Ti:Sapphire pump laser only makes one single pass through the Cs gain cell, there is no counter propagating pump beam, and the pump beam propagation was treated by simply applying the beam propagation method for a one-way propagation without iteration of the beam propagation calculation.

The further iteration between the calculation for the pump laser beam and the calculation for the signal laser beam was conducted in the way described in the previous section in this paper.

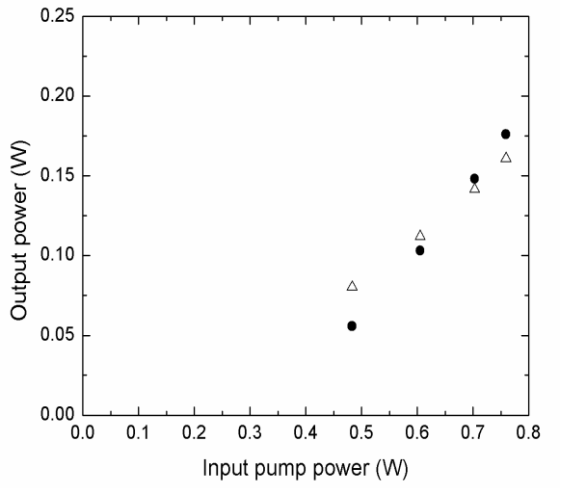

Fig. 2. The calculated output laser power (open triangles) versus the input pump power before entering the Cs cell, together with the experimental results (solid circles) presented in [1]. The output coupler reflectivity used in the calculation and in the experiment is 0.5.

As stated in [1] the one-way cavity transmission, excluding output coupler loss, of about 0.82 was measured at 894.6 nm with the cell cooled to room temperature to avoid significant Cs absorption. This cavity loss is understood to be due to the reflection on the four uncoated window surfaces of the inner Cs cell (the window material is understood to have a refractive index of about 1.47) and the loss on the polarizer. Accordingly, in the computation the loss of laser power after each pass through the polarizer was properly set, and the transmission of laser power on each of the four uncoated window surfaces of the inner Cs cell was also properly set, so that the one-way cavity transmission at 894.6 nm, excluding output coupler loss, was about 0.82 when there is no Cs vapor in the cell. The pump laser is understood to be a TEM_{00} Gaussian beam focused to the center of the Cs cell along the laser axis when there is no Cs vapor in the cell (the distance between the beam waist and the left cell window is the same as the distance between the beam waist and the right cell window), and the beam waist radius is 75 μm at $1/e^2$ of the axial intensity when there is no Cs vapor in the cell. The pump power is measured just before it enters the Cs cell and is delivered into the cell with an efficiency of 0.9 from that point.

#152299 - $15.00 USD Received 3 Aug 2011; revised 2 Sep 2011; accepted 3 Sep 2011; published 26 Sep 2011

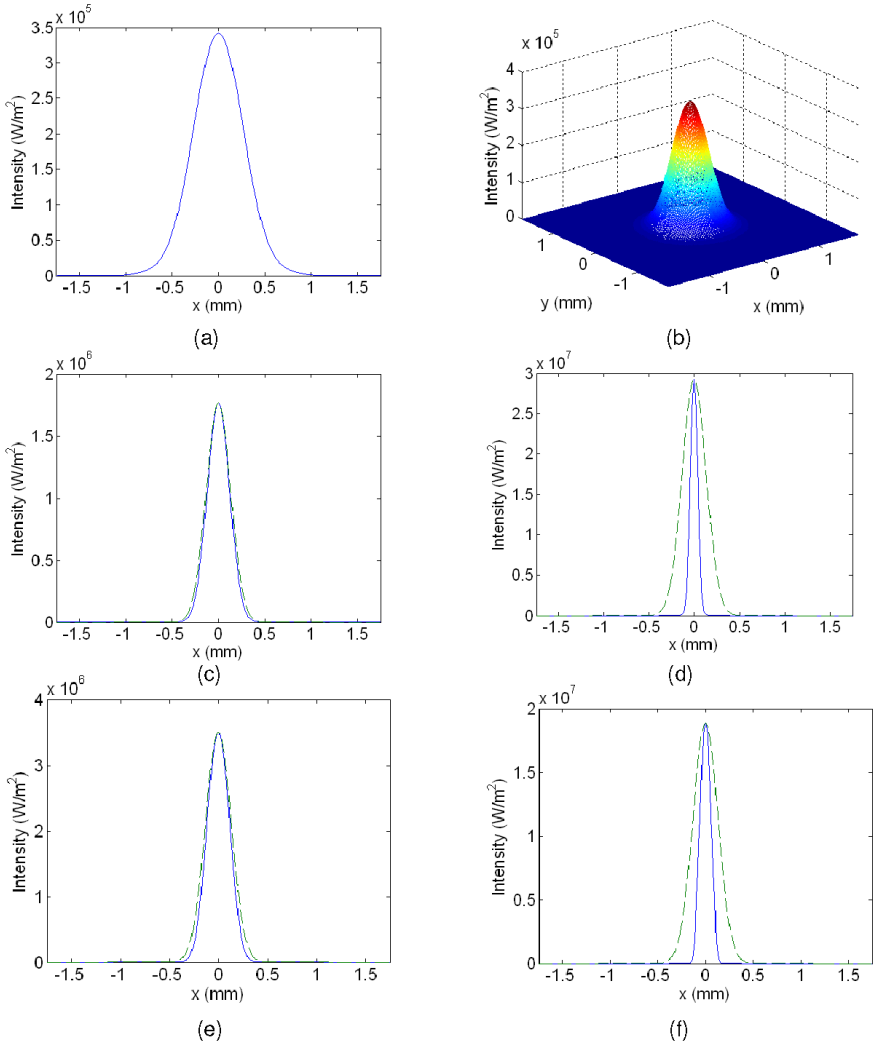

Fig. 3. (a) Output laser intensity as a function of the x coordinate for y = 0 just after passing the output coupler; (b) output laser intensity in the transverse x-y plane; (c) intensity of the laser before entering the Cs cell from the left window; (d) intensity of the laser before leaving the Cs cell from the right window; (e) intensity of the laser before entering the Cs cell from the right window; (f) intensity of the laser before leaving the Cs cell from the left window. The solid lines represent the calculated laser intensity; the dashed lines in (c), (d), (e) and (f) represent the intensity pattern of a TEM_{00} Gaussian beam right at its beam waist with the beam waist radius of 262.5 μm at $1/e^2$ of the axial intensity, and are scaled for comparison with the numerical calculation.

The numerical calculation confirmed that the considered laser operates in single spatial mode although it is different from the passive cavity mode. Shown in Fig. 2 is the plot of the calculated output laser power as a function of the input pump power before entering the Cs cell using an output coupler reflectivity of 0.5, together with the experimental results presented in [1]. The difference in the slope efficiency between the calculation and the experiment is possibly caused by the estimate of cavity loss being not accurate and a small amount of the laser power reflected back into the Cs gain medium by the uncoated cell windows which might be amplified. This small amount of reflected laser power was not properly included in the numerical calculation since we were not certain if this power eventually entered the laser output or somehow escaped from the cavity. Other possible

#152299 - $15.00 USD Received 3 Aug 2011; revised 2 Sep 2011; accepted 3 Sep 2011; published 26 Sep 2011

factors that may cause the difference between the calculation and the experiment include: (1) some material parameters might not be accurate and (2) there might be experimental uncertainties.

After the solution converges the laser intensity at different places inside and outside the resonator can be obtained easily. Shown in Fig. 3 are the plots of the calculated laser intensity at different places for the laser considered for input pump power equal to 0.759 W.

From Fig. 3 it can be seen that in steady state operation the spatial intensity pattern of the laser beam changes significantly each time it passes through the gain cell. This is different from the results presented in [1], where it is stated that at the location of the Cs cell the developed laser radiation had a beam waist of 263 μm. In addition, in Table 3 in [1] it is shown that the measured beam waist of the laser ($1/e^2$ intensity radius) is $W_L = 262.5\ \mu m$. From Fig. 3 (c) it can be seen that in steady state operation the laser beam propagating rightward at the left cell window is quite close to a Gaussian beam with beam waist of 262.5 μm. However, from Fig. 3 (d) it can be seen that the transverse size of the laser beam is significantly reduced after it passes through the gain cell. Figures 3 (e) and (f) show that when the laser beam is reflected by the high reflector and reaches the right cell window it is again quite close to a Gaussian beam with beam waist of 262.5 μm, but its transverse size is reduced again after it passes the gain cell traveling to the left. The reason for the decrease in the transverse size of the laser beam each time it passes the Cs cell is because the pumped region is relatively small (the pump beam waist radius at the cell center is 75 μm at $1/e^2$ of the axial intensity when there is no Cs vapor), and laser power is absorbed by Cs vapor where there is little or no pump power.

When the solution converged, after passing through the Cs vapor the pump power is reduced to about 0.00826 W right before passing the right cell window when the input pump power before entering the Cs cell is 0.759 W. This corresponds to an effective pump absorption efficiency of about 98.8%. To see how lasing changes the pump absorption, the laser intensity was set to zero and the same pump laser with the power of 0.759 W before entering the cell was numerically propagated through the cell. After passing the Cs vapor the pump laser power was reduced to about 0.491 W before passing the right cell window. This corresponds to an effective pump absorption efficiency of about 28%. It can be seen that in the considered Cs laser the pump absorption efficiency is significantly higher in steady state laser operation than that without lasing. The reason for this is because the emission of laser photons by the alkali atoms through stimulated laser emission causes transition of the alkali atoms from the upper laser level to the ground level (level 1), and this makes more atoms available to absorb the pump photons. The absorbed pump distribution is also different in steady state laser operation compared to the situation without laser.

As described previously in this paper, the transverse size of the pumped region is relatively small, and laser power could be absorbed by the Cs vapor where there is not much pump power. The absorption of laser power in the outer region of the laser beam could decrease the total laser efficiency. In addition, in [3] an optimal ratio between the sizes of the pump beam and the laser cavity mode was experimentally determined for the laser system presented there. It is also stated in [3] that the ratio of the pump beam waist to the laser cavity mode waist is important for three level lasers because it determines the re-absorption losses, absorption at the laser wavelength. To investigate this phenomenon in more detail for the laser considered here the transverse size of the pump beam (pumped region) was varied and the calculation was carried out again. The input pump power before entering the Cs cell was fixed at 0.759 W. All the other parameters are the same as those used in the calculation for Fig. 2. The pump laser is still TEM_{00} Gaussian beam focused to the center of the Cs cell along laser axis when there is no Cs vapor in the cell, and the distance between the beam waist and the left cell window is the same as the distance between the beam waist and the right cell window. In the calculation the input pump beam size was varied, and several different pump beam waist radii were used. Shown in Fig. 4 is the plot of the calculated output laser power versus the pump beam waist radius. Note that the pump beam waist radius in Fig. 4 is the one when there is no Cs vapor in the cell. From Fig. 4 it can be seen that the highest laser

#152299 - $15.00 USD Received 3 Aug 2011; revised 2 Sep 2011; accepted 3 Sep 2011; published 26 Sep 2011

efficiency can be achieved when the pump beam waist radius is somewhere around 135 μm. Therefore, for the experiment described in Ref [1]. the optimal pump beam waist radius would be somewhere around 135 μm.

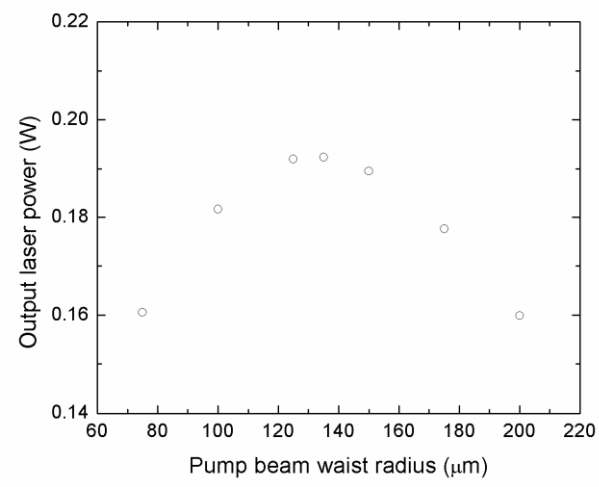

Fig. 4. The calculated output laser power versus the pump beam waist radius at $1/e^2$ of the axial intensity.

Finally, for the pump beam waist radius fixed at 135 μm, the location of the beam waist for the TEM_{00} Gaussian pump beam was shifted to both the left and right surfaces of the Cs gain medium (see Fig. 2 of [1] for the sketch of the Cs gain cell), and the calculation was carried out again. The pump beam waist radius and its waist location are again the ones when there is no Cs vapor in the cell. The other parameters are the same as those used in the calculation for Fig. 4. When the pump beam waist was located on the left surface of the Cs gain medium, the calculated output laser power is 0.193 W. When the pump beam waist was located on the right surface of the Cs gain medium, the calculated output laser power is 0.191 W. Compared to 0.192 W which is the calculated output laser power with the pump beam waist located in the center of the Cs cell along laser axis (the one shown in Fig. 4), it can be seen that the shift of the pump beam waist to either the left or right surfaces of the Cs gain medium doesn't change the output laser power significantly for pump beam waist radius fixed at 135 μm.

Further in-depth investigation into the general problem of analyzing and optimizing alkali vapor lasers (either laser resonators or amplifiers) remains very interesting. These would include further analyses of the interaction of laser beam with resonator (and the optical components inside the resonator), gain medium, and pump, as well as further analyses of the reshaping (as already demonstrated in this paper) of both signal laser beam and pump beam (or absorbed pump distribution) in this type of three level gain medium. Diode laser pump sources [6], [11] would be good candidates for pump sources, which generally have a multiple transverse mode output instead of a diffraction-limited TEM_{00} mode output. Particularly, in Ref [6]. a spectrally narrowed diode laser system is described with spectral width of only 10 GHz, which is less than the collision broadened spectral width of absorption in the Cs vapor described in Ref [1]. Therefore, pumping with the spectrally narrowed diode laser described in [6] would have an improved spectral overlap between pump radiation and absorption in the Cs vapor described in [1], compared to pumping with the Ti:Sapphire laser described in [1] which has a spectral width of ~30 GHz. As outcomes of analyzing this type of three level lasers, especially in more general configurations, a very useful tool can be established for designing and implementing such systems, and extensive investigation can be done on diode laser pumped alkali vapor lasers.

#152299 - $15.00 USD Received 3 Aug 2011; revised 2 Sep 2011; accepted 3 Sep 2011; published 26 Sep 2011

4. Conclusion

Detailed numerical analyses were conducted for a published single spatial mode Cs laser pumped by a diffraction-limited Ti: Sapphire laser. These analyses were made possible by the successful application of a computation model initially developed for analyzing solid state lasers. The details of how the computation is performed, and the convergence behavior of the computation, are also described and discussed. In the laser studied the spatial pattern of the laser beam is shown to be quite different from that of the passive cavity mode. According to the calculation, pump absorption is more efficient and the absorbed pump distribution is different in the presence of laser light compared to the situation without laser light. It is also demonstrated that changing the transverse size of the pump beam could change the laser efficiency for the considered laser system. Shifting the pump beam waist location was also studied. Although the analyses were carried out for a specific Cs laser the conclusions should be general for other alkali vapor lasers. This work provides a starting point for further investigation in modeling and understanding alkali metal vapor lasers and similar systems, especially in more general configurations.

Acknowledgments

The authors thank the financial support of Trumpf, Inc. We also thank Raymond J. Beach of the Lawrence Livermore National Laboratory for several discussions of the work presented in Ref. [1].

#152299 - $15.00 USD Received 3 Aug 2011; revised 2 Sep 2011; accepted 3 Sep 2011; published 26 Sep 2011